BioOne COMPLETE

Feasibility of Retrieving Land Surface Heat Fluxes from ASTER Data Using SEBS: a Case Study from the NamCo Area of the Tibetan Plateau

Authors: Ma, Weiqiang, Ma, Yaoming, and Su, Bob

Feasibility of Retrieving Land Surface Heat Fluxes from ASTER Data Using SEBS: a Case Study from the NamCo Area of the Tibetan Plateau

Weiqiang Ma†§
Yaoming Ma† and*
Bob Su‡

*Laboratory of Tibetan Environment Changes and Land Surface Processes, Institute of Tibetan Plateau Research, Chinese Academy of Sciences, Beijing 100085, China
†Key Laboratory of Land Surface Process and Climate Change in Cold and Arid Regions, Cold and Arid Regions Environmental and Engineering Research Institute, Chinese Academy of Sciences, Lanzhou 730000, Gansu, China
‡Faculty of Geo-Information Science and Earth Observation, University of Twente, Enschede P.O. Box 6, 7500 AA, Netherlands
§Corresponding author: wqma@lzb.ac.cn or wqmacn@gmail.com

Abstract

Surface fluxes are important boundary conditions for climatological modeling and the Asian monsoon system. The recent availability of high-resolution, multi-band imagery from the ASTER (Advanced Space-borne Thermal Emission and Reflection radiometer) sensor has enabled us to estimate surface fluxes to bridge the gap between local-scale flux measurements using micrometeorological instruments and regional scale land-atmosphere exchanges of water and heat fluxes that are fundamental for the understanding of the water cycle in the Asian monsoon system. A Surface Energy Balance System (SEBS) method based on ASTER data and field observations has been proposed and tested in this paper for deriving net radiation flux (R_n), soil heat flux (G_0), sensible heat flux (H), and latent heat flux (λE) over a heterogeneous land surface. As a case study, the methodology was applied to an experimental area at NamCo, located at the central Tibetan Plateau, China. The ASTER data of 11 June 2006, 29 October 2007, and 25 February 2008 was used in this paper for the NamCo area case. To validate the proposed methodology, the ground-measured land surface heat fluxes (net radiation flux (R_n), soil heat flux (G_0), sensible heat flux (H), and latent heat flux (λE)) were compared to the ASTER derived values. The results show that the derived land surface heat fluxes in different months over the study area are in good accordance with the land surface status. The tendency is basically to maintain consistency. It is therefore concluded that the proposed methodology is successful for the retrieval of land surface heat fluxes using the ASTER data and filed observations over the study area.

Introduction

The energy and water cycles play an important role in the Asian monsoon system over the Tibetan Plateau. The Tibetan Plateau contains the world's highest elevation with an average elevation for relief features of about 4000 m. It represents an extensive mass extending from subtropical to middle latitudes and spans more than 25° of longitude. Because of its topographic character, the plateau surface absorbs a large amount of solar radiation energy (much of which is redistributed by cryospheric processes), and undergoes dramatic seasonal changes of surface heat and water fluxes (e.g., Ye and Gao, 1979; Ye, 1981; Yanai et al., 1992; Ye and Wu, 1998; Ma et al., 2002, 2006; Ma and Tsukamoto, 2002). Some interesting detailed studies concerning the land surface heat fluxes have been reported in the northern Tibetan Plateau (e.g., Yang et al., 2002, 2003; Ma et al., 2002; Choi et al., 2004; Zuo et al., 2005; Ma and Ma, 2006). These researches were, however, on point-level or a local-patch-level. Since land-surface atmosphere interaction information is required for this area, the aggregation of the individual results into a regional scale is necessary.

Remote sensing offers the possibility to derive regional distribution of land surface heat fluxes over a heterogeneous land surface in combination with sparse field experimental stations. Remote sensing data provided by satellites are a means of obtaining consistent and frequent observations of spectral albedo and emittance of radiation at elements in a patch landscape and on a global scale (Sellers et al., 1990). The land surface variables and vegetation variables, such as surface temperature (T_{sfc}), surface hemispherical albedo (r_0), *NDVI*, *MSAVI*, *LAI*, and surface thermal emissivity (ε) can be derived directly from satellite observations (e.g., Susskind et al., 1984; Che'din et al., 1985; Tucker, 1986; Wan and Dozier, 1989; Menenti et al., 1989; Becker and Li, 1990, 1995; Watson et al., 1990; Baret and Guyot, 1997; Price, 1992; Kahle and Alley, 1992; Li and Becker, 1993; Qi et al., 1994; Norman et al, 1995; Schmugge et al., 1995; Kustas and Norman, 1997; Sobrino and Raissouni, 2000; Su, 2002; Ma et al., 2003a, 2003b; Oku and Ishikawa, 2004; Kato and Yamaguchi, 2005). The regional heat fluxes can be determined indirectly with the aid of these land surface variables and vegetation variables (Pinker, 1990).

Recent studies have explored several approaches to estimate the regional distribution of surface heat fluxes. These methods require specification of the vertical temperature difference between the surface temperature and the air temperature and an exchange resistance (e.g., Kustas et al., 1989; Kustas, 1990; Wang et al., 1995; Menenti et al., 1991; Menenti and Choudhury, 1993; Bastiaanssen, 1995; Kustas and Norman, 1997; Su, 2002). However, these remote sensing retrieval methods have been performed in homogeneous moist or semiarid regions, and investigations in heterogeneous landscapes of high altitude (e.g., the Tibetan Plateau area) are rare.

NOAA/AVHRR, GMS, and Landsat-7 ETM data have been used to determine regional land surface heat fluxes over the heterogeneous landscape of the Tibetan Plateau (Ma et al., 2003a, 2003b, 2005, 2006; Oku et al., 2007). However, the resolution of
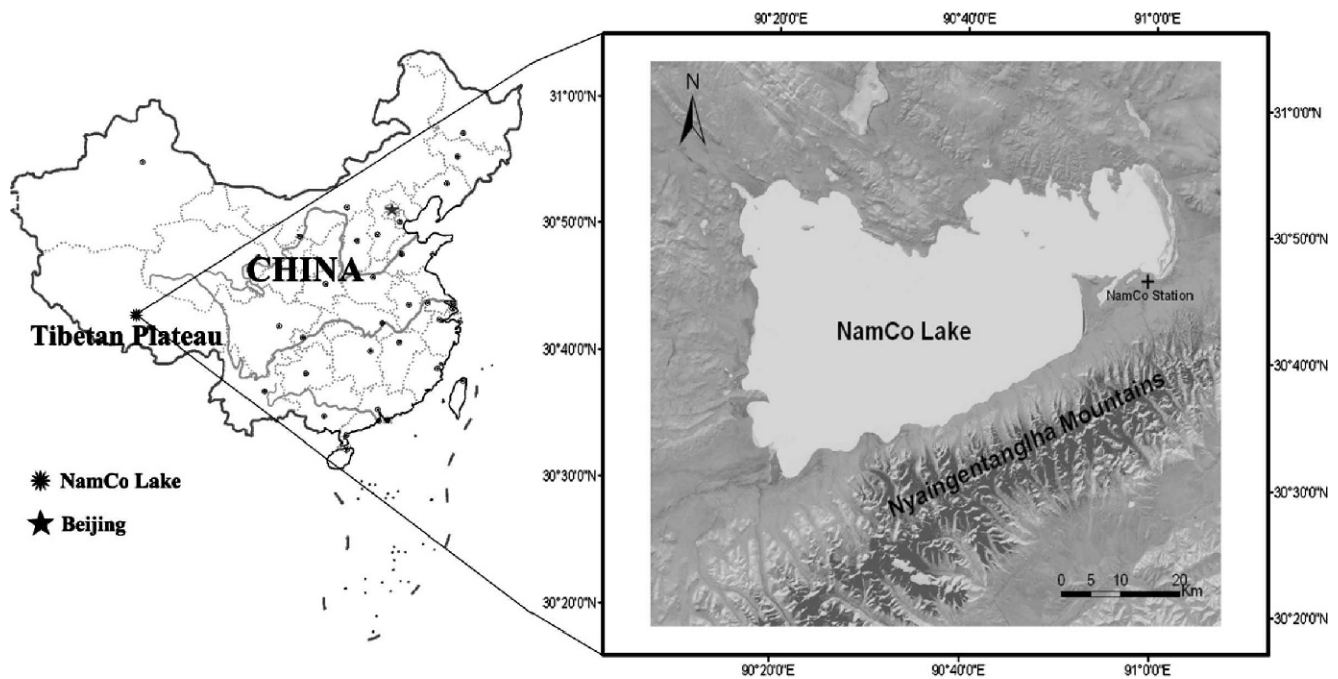
FIGURE 1. The goal of the study was to retrieve land surface heat fluxes using the NamCo area in the central Tibetan Plateau area of China. On the right is a Landsat TM map of the study area (Source for this data set was the Global Land Cover Facility at the University of Maryland; http://www.landcover.org.), including NamCo Lake and NamCo Station (compare with Fig. 3). Elevations in this area range from 4718 m for NamCo Lake and 4730 m at NamCo Station up to 7111 m in the mountains to the southeast. The location of NamCo Lake within China is shown in the sketch map on the left. Dots are major cities within China, and the dashed line shows the limits of claimed Chinese territory.

the NOAA/AVHRR and GMS data is about 1 km × 1 km and sub-pixel heterogeneity has been omitted. This is also the case with Landsat-7 ETM data. The aim of this research is to upscale *in situ* point observations of land surface variables and land surface heat fluxes to the regional scale using high-resolution (15 m × 15 m) ASTER data.

Data and Methodology

DATA

The recent availability of high-resolution, multi-band imagery from the ASTER sensor has enabled us to estimate surface fluxes. ASTER covers a wide spectral region with 14 bands from the visible to the thermal infrared with high spatial, spectral, and radiometric resolution. The spatial resolution varies with wavelength: 15 m in the visible and near-infrared (VNIR, 0.52–0.86 μm), 30 m in the shortwave infrared (SWIR, 1.6–2.43 μm), and 90 m in the thermal infrared (TIR, 8.1–11.6 μm) (Yamaguchi et al., 1998).

The most relevant data, collected at the NamCo station (Ma et al., 2008) to support the parameterization of land surface heat fluxes and analysis of ASTER images in this paper, consist of surface radiation budget components, surface radiation temperature, surface albedo, humidity, wind speed and direction measured at the Atmospheric Boundary Layer (ABL) tower; turbulent fluxes measured by the eddy correlation (EC) technique; soil heat flux; soil temperature profiles; soil moisture profiles; and the vegetation state (Fig. 1). The sensible heat flux and latent heat flux using EC system is made by Campbell (CSAT3). So far, EC has been recognized as the best measurement tool for sensible heat flux and latent heat flux. The measurement resolution: u_x and u_y are 1 mm/s rms; u_z is 0.5 mm/s rms; c is 15 mm/s (0.025 °C) rms. Accuracy assumes −30 to +50 °C range; wind speeds <30 m/s; and wind angles of ±170°.

THEORY AND SCHEME

A Surface Energy Balance System (SEBS; Su, 2002) was proposed for the estimation of atmospheric turbulent fluxes and evaporative fraction using satellite earth observation data, in combination with meteorological information at proper scales. SEBS consists of: a set of tools for the determination of the land surface physical parameters, such as surface albedo, emissivity, surface temperature, vegetation coverage, etc., from spectral reflectance and radiance measurements; it is a model for the determination of the roughness length for heat transfer (Su, 2002).

In this study, the SEBS retrieval algorithm is used for the ASTER data. The general concept of the methodology is shown in a diagram (Fig. 2). The surface albedo for shortwave radiation (r_0) is retrieved from narrowband-broadband conversion by Liang (Liang, 2001). The land surface temperature (T_{sfc}) is derived using a method developed by Juan et al. (2006) from multispectral thermal infrared data. Juan et al. (2006) also evaluated a technique to extract emissivity information from multispectral thermal infrared data adding vegetation information. The radiative transfer model SMAC (Rahman and Dedieu, 1994) computes the downward shortwave and longwave radiation at the surface. With these results the surface net radiation flux (R_n) is determined. On the basis of the field observations, the soil heat flux (G_0) is estimated from net radiation flux (R_n). The sensible heat flux (H) is estimated from T_{sfc}, and regional latent heat flux (λE) is derived as the residual of the energy budget theorem (Liou, 2004; Ma et al., 2006) for land surface.

The net radiation flux R_n is estimated as

$$R_n(x,y) = K_\downarrow(x,y) - K_\uparrow(x,y) + L_\downarrow(x,y) - L_\uparrow(x,y)$$
$$= (1 - r_0(x,y)) \cdot K_\downarrow(x,y) + L_\downarrow(x,y) - \varepsilon_0(x,y)\sigma T_{sfc}^4(x,y) \quad (1)$$

where $\varepsilon_0(x,y)$ is surface emissivity, $K_\downarrow$ (Wm^{-2}) represents the
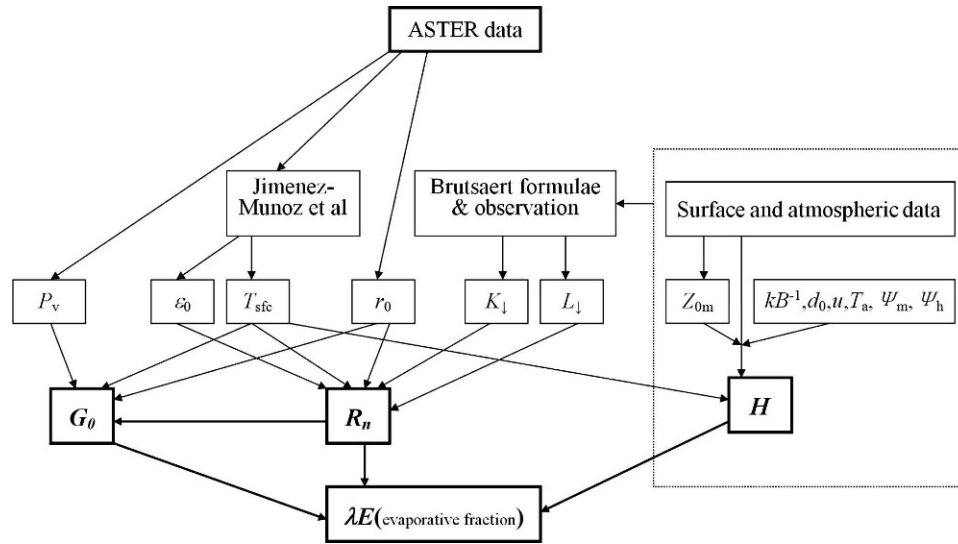
FIGURE 2. Diagram of parameterization procedure by combining Advanced Space-borne Thermal Emission and Reflection radiometer (ASTER) data with field observations. The method of Jimenez-Munoz et al. (2006) yields land surface temperature and emissivity. SMAC is radiative transfer model; P_v is vegetation coverage; ε_0 is emissivity; T_{sfc} is land surface temperature; r_0 is land surface albedo for shortwave radiation; $K\downarrow$ is shortwave radiation; $L\downarrow$ is longwave radiation; Z_{0m} is roughness height for momentum transfer; kB^{-1} is the excess resistance for heat transportation; d_0 is zero plane displacement height; u is mean wind speed; T_a is air temperature; Ψ_m is stability correction function for momentum; Ψ_h is stability correction function for sensible heat transfer; G_0 is the soil heat flux; R_n is the net radiation flux; λE is the regional latent heat flux; and H is the sensible heat flux.

shortwave (0.3–3 μm), and $L\downarrow$ (Wm^{-2}) the longwave (3–100 μm) radiation components, respectively. Surface albedo $r_0(x,y)$ is derived from the narrowband-broadband conversion method by Liang (2001). Since ASTER has nine bands, it is expected that so many bands should enable us to convert narrowband to broadband albedos effectively. Liang (2001) found that the conversions are quite linear. The resultant linear equations are collated as follows:

$$r_0 = 0.484\alpha_1 + 0.335\alpha_3 - 0.324\alpha_5 + 0.551\alpha_6 + 0.305\alpha_8 \\ - 0.367\alpha_9 - 0.0015 \quad (2)$$

where i (i = 1–9) are the correspondent ASTER band surface reflectances.

The equation to calculate soil heat flux is parameterized as (Su, 2002):

$$G_0 = R_n[\Gamma_c + (1-f_c)\cdot(\Gamma_s - \Gamma_c)] \quad (3)$$

in which it is assumed that the ratio of soil heat flux to net radiation $\Gamma_c = 0.05$ for the full vegetation canopy (Monteith, 1973), and $\Gamma_s = 0.315$ for bare soil (Kustas et al., 1989). An interpolation is then performed between these limiting cases using the fractional canopy coverage, f_c.

In order to derive the sensible and latent heat flux, similarity theory (Monin and Obukhov, 1954) will be used here. In ASL (Atmospheric Surface Layer), the similarity relationships for the profiles of the mean wind speed, u, and the mean temperature, $\theta_0 - \theta_a$, are usually written in integral form as (Monin and Obukhov, 1954):

$$u = \frac{u_*}{k}\left[\ln\left(\frac{z-d_0}{z_{om}}\right) - \Psi_m\left(\frac{z-d_0}{L}\right) + \Psi_m\left(\frac{z_{0m}}{L}\right)\right] \quad (4)$$

$$\theta_0 - \theta_a = \frac{H}{ku_*\rho C_p}\left[\ln\left(\frac{z-d_0}{z_{oh}}\right) - \Psi_h\left(\frac{z-d_0}{L}\right) + \Psi_h\left(\frac{z_{0h}}{L}\right)\right] \quad (5)$$

where z is the height above the surface, $u_* = (\tau_0/\rho)^{1/2}$ is the friction velocity, τ_0 is the surface shear stress, ρ is the density of air, $k = 0.4$ is von Karman's constant, d_0 is the zero plane displacement height, z_{0m} is the roughness height for momentum transfer, θ_0 is the potential temperature at the surface, θ_a is the potential air temperature at height z, z_{0h} is the scalar roughness height for heat transfer, ψ_m and ψ_h are the stability correction functions for momentum and sensible heat transfer, respectively. L is the Obukhov length defined as (Monin and Obukhov, 1954):

$$L = \frac{\rho C_p u_*^3 \theta_v}{kgH} \quad (6)$$

where g is the acceleration due to gravity and θ_v is the potential virtual temperature near the surface.

Normally the latent heat flux λE is the residual resulting from an application of the energy budget theorem to the land surface (Ma et al, 2006):

$$\lambda E = R_n - H - G_0 \quad (7)$$

but SEBS use the evaporative fraction to derived latent heat flux, which is estimated by:

TABLE 1

The input observation data of the Surface Energy Balance System (SEBS).

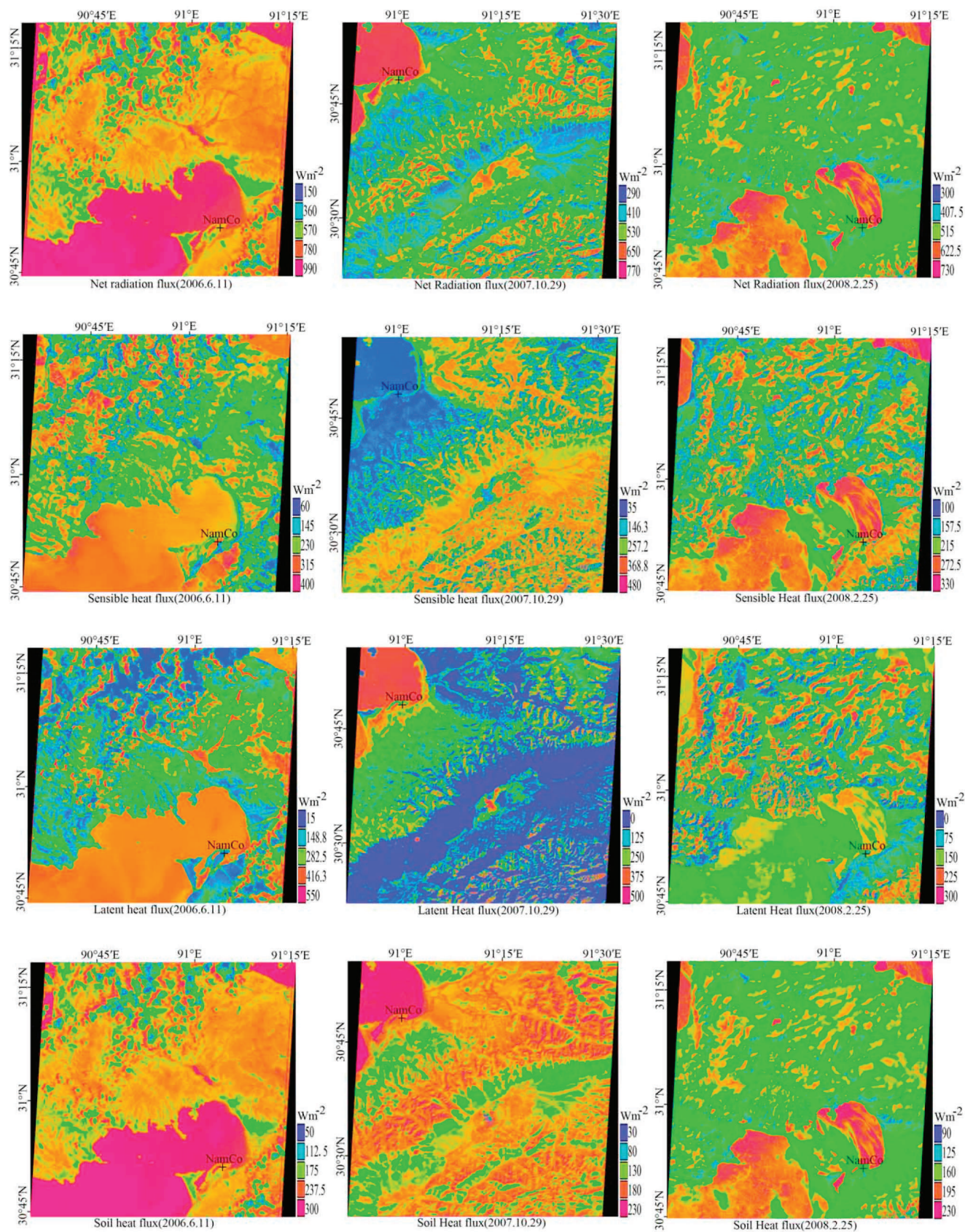|	Humidity (kg kg^{-1})	Wind speed (m s^{-1})	Air temperature (°C)	Pressure at surface (hPa)
11 June 2006	0.006	5.8	13.2	570
29 October 2007	0.006	1.5	2.6	572.8
25 February 2008	0.006	5.5	−5	565

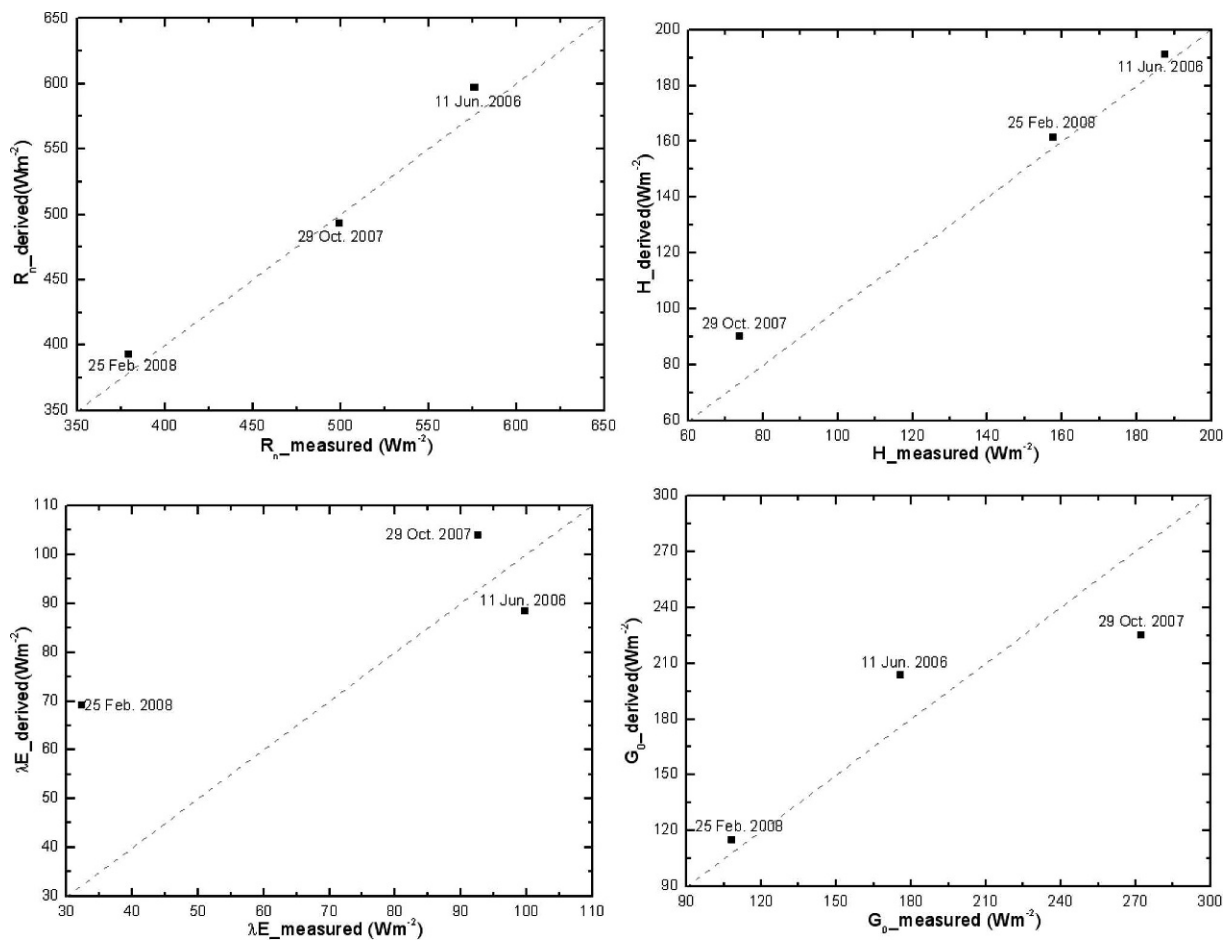**FIGURE 3.** Distribution maps of land surface heat fluxes over the area around NamCo Station (compare with Fig. 1).

FIGURE 4. Validation of the derived net radiation (R_n), soil heat flux (G_0), sensible heat flux (H), and latent heat flux (λE) against ground measurements over the NamCo station with 1:1 line. Observation time: 12:40 (Beijing Time).

$$\Lambda = \frac{\lambda E}{R_n - G} \qquad (8)$$

The latent heat flux (λE) can then be calculated by

$$\lambda E = \Lambda(R_n - G_0) \qquad (9)$$

Case Studies and Validation

As a case study, three scenes of ASTER data over the NamCo area of the Tibetan Plateau are used here. Table 1 shows the input data of SEBS. Figure 3 shows the distribution maps of surface heat fluxes around the NamCo area. Figure 4 shows the validation of the derived net radiation R_n, soil heat flux G_0, sensible heat flux H, and latent heat flux λE against ground measurements over the NamCo area with a 1:1 line.

The results show the following:

(1) The derived surface heat fluxes (net radiation flux R_n, soil heat flux G_0, sensible heat flux H, and latent heat flux λE) in different months over the study area are in good accordance with the land surface status. The experimental area includes a variety of land surfaces such as a large area of grassy marshland, some desertification grassland areas, many small rivers and NamCo lake; therefore, these derived parameters show a wide range due to the strong contrast of surface features. Net radiation flux changed from 300 to 730 W m^{-2} in February, from 150 to 990 W m^{-2} in June, and from 290 to 770 W m^{-2} in October. Soil heat flux varied from 90 to 230 W m^{-2} in February, from 50 to 300 W m^{-2} in June, and from 30 to 230 W m^{-2} in October. Sensible heat flux ranged from 100 to 330 W m^{-2} in February, from 60 to 400 W m^{-2} in June, and from 35 to 480 W m^{-2} in October. Latent heat flux varied from 0 to 300 W m^{-2} in February, from 15 to 550 W m^{-2} in June, and from 0 to 500 W m^{-2} in October (see Fig. 3).

(2) The derived net radiation flux over the study area is very close to the field measurements; the absolute percent difference (APD) is 3.5%, which is the result of improvement in surface albedo and surface temperature. The regional soil heat flux derived from the relationship between soil heat flux and net radiation flux is suitable for heterogeneous land surface of the NamCo area, because the relationship itself was derived from the same area.

(3) The derived regional sensible heat flux and latent heat flux at the validation sites in the NamCo area are in good agreement with field measurements (Fig. 4). Although it has a deviation, it may also reflect the surface status in the NamCo area. This is due to the fact that atmospheric boundary layer processes have been considered in more detail in our methodology, and the proposed parameterization for sensible heat flux and latent heat flux can be used over the NamCo area. In Table 1 the input observation data can be seen clearly.

Concluding remarks

In this study, the regional distributions of land surface heat fluxes (net radiation flux, soil heat flux, sensible heat flux, and latent heat flux) over the heterogeneous central Tibetan Plateau area were derived with the aid of ASTER data and field observations. Reasonable results of land surface heat fluxes were gained in this study.

The retrieval of regional land surface heat fluxes over a heterogeneous landscape is not an easy task.

(1) Only three ASTER images are used in this study. To obtain more accurate regional land surface fluxes (daily to seasonal variations) over a larger area (the Tibetan Plateau), more field observations (ABL tower and radiation measurement system, radiosonde system, turbulent fluxes measured by the eddy correlation technique, soil moisture and soil temperature measurement system, etc.) and other satellite sensors such as MODIS (Moderate Resolution Imaging Spectroradiometer) and NOAA (National Oceanic and Atmospheric Administration)/AVHRR (Advanced Very High Resolution Radiometer) with more frequent temporal coverage have to be used.

(2) This study implies the SEBS method is only applicable to clear-sky days. In order to extend its applicability to cloudy skies, we should consider using microwave remote sensing data to derive surface temperature and other land surface variables.

SEBS has been developed to estimate atmospheric turbulent fluxes using satellite earth observation data, in combination with meteorological data from a proper reference height given by either *in situ* measurements for application to a point, or radiosonde or meteorological forecasts for application at larger scales. On the basis of these experimental validations, SEBS can be used to estimate turbulent heat fluxes at different scales with acceptable accuracy.

Acknowledgments

References Cited

Baret, F., and Guyot, G., 1997: Potentials and limits of vegetation indices for LAI and APAR assessment. *Remote Sensing of Environment*, 35: 161–173.

Bastiaanssen, W. G. M., 1995: Regionalization of Surface Flux Densities and Moisture Indicators in Composite Terrain. Ph.D. thesis. Wageningen Agricultural University, Wageningen, Netherlands, 143–161.

Becker, F., and Li, Z.-L., 1990: Towards a local split window method over land surfaces, *International Journal of Remote Sensing*, 11: 369–393.

Becker, F., and Li, Z.-L., 1995: Surface temperature and emissivity at various scales: definition, measurement and related problems. *Remote Sensing Reviews*, 12: 225–253.

Che'din, A., Scott, N. A., Wahiche, C., and Moulinier, P., 1985: The improved initialisation inversion method: a high resolution physical method for temperature retrievals from Tiros-N series. *Journal of Climate and Applied Meteorology*, 24: 124–143.

Choi, T., Hong, J., Kim, J., Lee, H., Asanuma, J., Ishikawa, H., Tsukamoto, O., Zhiqui, G., Ma, Y., Ueno, K., Wang, J., Koike, T., and Yasunari, T., 2004: Turbulent exchange of heat, water vapor, and momentum over a Tibetan prairie by eddy covariance and flux variance measurements. *Journal of Geophysical Research*, 109: article D21106, doi:10.1029/2004JD004767.

Jiménez-Muñoza, J. C., Sobrino, J., Gillespie, A., Sabolb, D., and William, T., 2006: Improved land surface emissivities over agricultural areas using ASTER NDVI. *Remote Sensing of Environment*, 103: 474–487.

Kahle, A. B., and Alley, R. E., 1992: Separation of temperature and emittance in remotely sensed radiance measurements. *Remote Sensing of Environment*, 42: 107–112.

Kato, S., and Yamaguchi, Y., 2005: Analysis of urban heat-island effect using ASTER and ETM+ data: separation of anthropogenic heat discharge and natural heat radiation from sensible heat flux. *Remote Sensing of Environment*, 99: 44–54.

Kustas, W. P., 1990: Estimates of evapotranspiration with a one- and two-layer model of heat transfer over partial canopy cover. *Journal of Applied Meteorology*, 29: 704–715.

Kustas, W. P., and Norman, J. M., 1997: A two-source approach for estimating turbulent fluxes using multiple angle thermal infrared observations. *Water Resources Research*, 33: 1495–1508.

Kustas, W. P., Choudhury, B. J., Moran, M. S., Reginato, R. J., Jackson, R. D., Gay, L. W., and Weaver, H. L., 1989: Determination of sensible heat flux over sparse canopy using thermal infrared data. *Agricultural and Forest Meteorology*, 44: 197–216.

Li, Z.-L., and Becker, F., 1993: Feasibility of land surface temperature and emissivity determination from AVHRR data. *Remote Sensing of Environment*, 43: 67–85.

Liang, S., 2001: Narrowband to broadband conversions of land surface albedo. *Remote Sensing of Environment*, 76: 213–238.

Liou, K. N., 2004: *An Introduction to Atmospheric Radiation*. 2nd edition. Beijing: China Meteorology Press.

Ma, W., and Ma, Y., 2006: The annual variations on land surface energy in the northern Tibetan Plateau. *Environmental Geology*, 50(5), doi:10.1007/s00254-006-0238-9.

Ma, Y., and Tsukamoto, O., 2002: *Combining Satellite Remote Sensing with Field Observations for Land Surface Heat Fluxes over Inhomogeneous Landscape*. Beijing: China Meteorology Press.

Ma, Y., Tsukamoto, O., Wang, J., Ishikawa, H., and Tamagawa, I., 2002: Analysis of aerodynamic and thermodynamic parameters over the grassy marshland surface of Tibetan Plateau. *Progress in Natural Science*, 12: 36–40.

Ma, Y., Su, Z., Koike, T., Yao, T., Ishikawa, H., Ueno, K., and Menenti, M., 2003a: On measuring and remote sensing surface energy partitioning over the Tibetan Plateau—From GAME/Tibet to CAMP/Tibet. *Physics and Chemistry of the Earth*, 28: 63–74.

Ma, Y., Ishikawa, H., Tsukamoto, O., Menenti, M., Su, Z., Yao, T., Koike, T., and Yasunari, T., 2003b: Regionalization of surface fluxes over heterogeneous landscape of the Tibetan Plateau by using satellite remote sensing. *Journal of the Meteorological Society of Japan*, 81: 277–293.

Ma, Y., Fan, S., Ishikawa, H., Tsukamoto, O., Yao, T., Koike, T., Zuo, H., Hu, Z., and Su, Z., 2005: Diurnal and inter-monthly variation of land surface heat fluxes over the central Tibetan Plateau area. *Theoretical and Applied Climatology*, 80: 259–273.

Ma, Y., Zhong, L., Su, Z., Ishikawa, H., Menenti, M., and Koike, T., 2006: Determination of regional distributions and seasonal variations of land surface heat fluxes from Landsat-7 Enhanced Thematic Mapper data over the central Tibetan Plateau area. *Journal of Geophysical Research*, 111: article D10305, doi:10.1029/2005JD006742.

Ma, Y., Kang, S. C., Zhu, L. P., Xu, B. Q., Tian, L., and Yao, T. D., 2008: Tibetan Observation and Research Platform atmosphere-land Interaction over a heterogeneous landscape. *Bulletin of the American Meteorological Society*, 89(10): 1487–1492.

Menenti, M., and Choudhury, B. J., 1993: Parameterization of land surface evaporation by means of location dependent potential evaporation and surface temperature range. *In* Bolle, H. J., Feddes, R. A., and Kalma, J. D. (eds.), *Exchange Processes at the Land Surface for a Range of Space and Time Scales* IAHS Publication, 212: 561–568.

Menenti, M., Bastiaanssen, W. G. M., and Van Eick, D., 1989: Determination of hemispheric albedo with Thematic Mapper data. *Remote Sensing of Environment*, 28: 327–337.

Menenti, M., Bastiaanssen, W. G. M., Hefny, K., and Abd El Karim, M. H., 1991. Mapping of ground water losses by evaporation in the Western Desert of Egypt., Wageningen, Netherlands: DLO Winand Staring Center, Report 43:, 1–116.

Monin, A. S., and Obukhov, A. M., 1954: Basic laws of turbulent mixing in the ground layer of the atmosphere. Trans. Geophys. Inst. Akad. Nauk. USSR, 151: 163–187.

Monteith, J. L., 1973: *Principles of Environmental Physics*. London: Edward Arnold Press, 241 pp.

Norman, J. M., Kustas, W. P., and Humes, K. S., 1995: A two-source approach for estimating soil and vegetation energy fluxes from observations of directional radiometric surface temperature. *Agricultural and Forest Meteorology*, 77: 263–293.

Oku, Y., and Ishikawa, H., 2004: Estimation of land surface temperature over the Tibetan Plateau using GMS data. *Journal of Applied Meteorology*, 43: 548–561.

Oku, Y., Ishikawa, H., and Su, Z., 2007: Estimation of land surface energy fluxes over the Tibetan Plateau using GMS data. *Journal of Applied Meteorology and Climatology*, 46: 183–195.

Pinker, R. T., 1990: Satellites and our understanding of the surface energy balance. *Palaeogeography Palaeoclimatology Palaeoecology*, 82: 321–342.

Price, J. C., 1992: Estimating vegetation amount from visible and near infrared albedo. *Remote Sensing of Environment*, 41: 29–34.

Qi, J., Chehbouni, A., Huete, A. R., Kerr, Y. H., and Sorooshian, S., 1994: A modified soil adjusted vegetation index. *Remote Sensing of Environment*, 48: 119–126.

Rahman, H., and Dedieu, G., 1994: SMAC: a simplified method for atmospheric correction of satellite measurements in the solar spectrum. *International Journal of Remote Sensing*, 15: 123–143.

Schmugge, T. J., Hook, S., and Kahle, A., 1995: TIMS observation of surface emissivity in HAPEX-Sahel. Paper presented at International Geoscience and Remote Sensing Symposium, Institute of Electrical and Electronics Engineers, Florence, Italy, July.

Sellers, P. J., Rasool, S. I., and Bolle, H. J., 1990: A review of satellite data algorithms for studies of the land surface. *Bulletin of the American Meteorological Society*, 71: 1429–1447.

Sobrino, J. A., and Raissouni, N., 2000: Toward remote sensing methods for land cover dynamic monitoring: application to Morocco. *International Journal of Remote Sensing*, 21(2): 353–366.

Su, Z., 2002: The Surface Energy Balance System (SEBS) for estimation of turbulent heat fluxes. *Hydrology and Earth System Sciences*, 6: 85–99.

Susskind, J., Rosenfield, J., Renter, D., and Chahine, M. T., 1984: Remote sensing of weather and climate parameters from HIRS2/MSU on TIROS-N. *Journal of Geophysical Research*, 89: 4677–4697.

Tucker, C. J. (ed.), 1986: Monitoring the grasslands of semi-arid Africa using NOAA AVHRR data. *International Journal of Remote Sensing*, 7(11): 1383–1622.

Wan, Z., and Dozier, J., 1989: Land surface temperature measurement from space: physical principles and inverse modelling. *IEEE Transactions on Geoscience and Remote Sensing*, 27: 268–278.

Wang, J., Ma, Y., Menenti, M., Bastiaanssen, W. G. M., and Mistsuta, Y., 1995: The scaling-up of processes in the heterogeneous landscape of HEIFE with the aid of satellite remote sensing, *Journal of the Meteorological Society of Japan*, 73: 1235–1244.

Watson, K., Kruse, F., and Hummer-Miler, S., 1990: Thermal infrared exploration in the Carlin trend. *Geophysics*, 55: 70–79.

Yamaguchi, Y., Kahle, A. B., Tsu, H., Kawakami, T., and Pniel, M., 1998: Overview of the Advanced Spaceborne Thermal Emission and Reflection Radiometer (ASTER). *IEEE Transactions on Geoscience and Remote Sensing*, 36(4): 1062–1071.

Yanai, M., Li, C., and Song, Z., 1992: Seasonal heating of the Tibetan Plateau and its effects on the evolution of the Asian summer monsoon. *Journal of the Meteorological Society of Japan*, 70: 319–351.

Yang, K., Koike, T., Fujii, H., Tamagawa, K., and Hirose, N., 2002: Improvement of surface flux parameterizations with a turbulence-related length. *Quarterly Journal of the Royal Meteorological Society*, 128B: 2073–2088.

Yang, K., Koike, T., and Yang, D., 2003: Surface flux parameterization in the Tibetan Plateau. *Boundary Layer Meteorology*, 116: 245–262.

Ye, D., 1981: Some characteristics of the summer circulation over the Qinghai-Xizang (Tibet) Plateau and its neighborhood. *Bulletin of the American Meteorological Society*, 62: 14–19.

Ye, D., and Gao, Y., 1979: *The Meteorology of the Qinghai-Xizang (Tibet) Plateau*. Beijing: Science Press, 278 pp. (in Chinese).

Ye, D., and Wu, G., 1998: The role of the heat source of the Tibetan Plateau in the general circulation. *Meteorology and Atmospheric Physics*, 67: 181–198.

Zuo, H., Hu, Y., Li, D., Lu, S., and Ma, Y., 2005: Seasonal transition and its boundary characteristics in Amdo area of Tibetan Plateau. *Progress in Natural Science*, 15: 239–245.